
Life Science Informatics Publications

Research Journal of Life Sciences, Bioinformatics, Pharmaceutical and Chemical Sciences

Journal Home page http://www.rjlbpcs.com/

RJLBPCS

ISSN 2454-6348

**Original Research Article** **DOI: 10.26479/2018.0406.01**

# GREEN SYNTHESIS OF GOLD NANOPARTICLES AND EVALUATION OF ITS CYTOTOXIC PROPERTY AGAINST COLON CANCER CELL LINE

**Arpita Dey, A Yogamoorthy, S M Sundarapandian***

Department of Ecology and Environmental Sciences, School of Life Sciences,

Pondicherry University, Puducherry, India.

**ABSTRACT:** The green synthesis of gold nanoparticles was mediated by aqueous extract of *Wedelia trilobata* leaves and in-vitro cytotoxic efficacy of synthesized gold nanoparticle against HCT 15 human colon cancer cell line was studied. Synthesis of nanoparticles was completed within 30-35 minutes of reaction at room temperature and structural properties of the particles were studied through standard characterization methods. Formation of gold nanoparticles was initially confirmed by a change in colour from light yellow to deep purple and the appearance of Surface Plasmon Resonance at 533nm in UV-Visible spectroscopy. The particles were mostly spherical, crystalline with face-centered cubic structure with 10-50 nm diameters, and they exhibited a high degree of agglomeration. Further, MTT (3-(4,5-dimethylthiazol-2-yl)-2,5-diphenyltetrazolium bromide) tetrazolium reduction assay was conducted using different concentrations of gold nanoparticles (25-500µg/ml). The gold nanoparticles showed dose-dependent toxicity and the efficiency was up to 30 percent on average.

**KEYWORDS:** Noble metal nanoparticles, Biosynthesis, Cell cytotoxicity, MTT assay.

**Corresponding Author: Dr. S M Sundarapandian*** Ph.D.

Department of Ecology and Environmental Sciences, School of Life Sciences,

Pondicherry University, Puducherry, India. Email Address: smspandian65@gmil.com

## 1.INTRODUCTION

Metals have attracted a great interest in nanoscience and applications owing to the properties they exhibit at nanometer scale much different from their bulk properties [1] and these unique properties can be fine-tuned by manipulating their size as well [2]. These features make them suitable for diverse applications in electrical, chemical, and biological fields [3]. The conventional chemical and

physical routes of nanoparticle (particles diameter in the range of 1-100 nanometer) synthesis involve toxic chemicals, high energy consumption and higher cost. Biosynthesis of nanomaterial has been proven encouraging as the synthesis is possible at room temperature, rapid, eco-friendly, biocompatible [4] and does not involve multiple steps in synthesis. Plants are encouraged over micro-organisms as the need to grow and preserve culture is not there and the chance of contamination is zero to very low as well as they are less time consuming [5]. The biomolecules in the plant extracts act as reductants as well as capping agents in the synthesis of nanoparticles. Several plants that have been used in synthesis have shown a fast rate of synthesis [6]. In spite of the fact that metal nanoparticles synthesis using plant extracts has been reported by many workers in different plants such as alfalfa [7,8], geranium [9,10], neem [11], lemongrass [12], *Emblica officinalis* [13], *Aloe vera* [14], *Cinnamomum camphora* [15], *Magnolia kobus* [16], *Rosa hybrida* [17], *Aloe barbadensis* [18], Olive leaf [19], *Panax ginseng* [3], *Eclipta prostrata* [20], *Ocimum sanctum* [21], *Ginkgo biloba* [22], *Nerium oleander* [23], *Garcinia indica* [24], still there is lot to explore about the potential and efficiency of the plants in synthesis of nanoparticles of different shape, size, and their suitability for different applications. Synthesis of nanoparticles of desired shape and size depends on various reaction parameters such as concentration of metal salt, concentration of biomass extract, pH of the reaction solution, temperature, incubation time [25], aeration, mixing ratio, redox conditions [4, 26] and nature of the solvent as well [21]. Gold (Au) is a block-d transition metal with a higher atomic number. The gold nanoparticles show high dispersion due to its very small size and large surface area. It's resistance to oxidation by air, moisture and soft acids as well as its biocompatible nature, makes it a suitable candidate for biological applications particularly in cell targeting, drug-delivery, biomolecular imaging, tumors detection, antimicrobial, cancer therapy, chemical and biological sensing and so on [25, 27] There are prior reports that gold nanoparticles being used in chemotherapy and cancer cell diagnosis [28], in-vitro cytotoxicity assay [23] and they also act as probe for microscopic study of cancer cells [29]. The cytotoxicity and antiproliferative effect of nanoparticles depend on the cell type, particle size, and concentration as reported by Zăhan et al. [30]. Priya & Iyer [29] reported a dose-dependent effect of the biosynthesized nanoparticles against MCF 7 breast cancer cell lines. *Wedelia trilobata* (L.) Hitchc. leaf has not been evaluated so far in the synthesis of gold nanoparticles and hence present study was undertaken. In the present study, green synthesis of gold nanoparticles (AuNPs) by the aqueous *W. trilobata* leaves extract was carried out and its anticancer property was assessed in HCT 15 colon cancer cell line.

## 2. MATERIALS AND METHODS

### 2.1. Materials

*Wedelia trilobata* (L.) Hitchc is a perennial plant native to tropical America widely naturalized in tropical areas and largely used as ornamental ground cover. The leaves of *W. trilobata* are known to contain tannins, flavonoids, terpenoids, phenols, saponins [31]. Fresh and healthy leaves of *W. trilobata* were collected from the campus of Pondicherry University and identified with the help of morphological characters. Gold (III) chloride trihydrate ($HAuCl_4. 3H_2O$), Dulbecco's Modified Eagle's medium (DMEM), fetal bovine serum (FVS), Dimethyl sulfoxide (DMSO), MTT (3-4,5-dimethylthiazol-2-yl)-2,5-diphenyltetrazolium bromide) tetrazolium was purchased from Hi-Media Laboratories Pvt. Ltd. Mumbai, India.

### 2.2.Preparation of Plant Extract

Plant leaves extract preparation and nanoparticle synthesis was done as described by Rather et al. [32] with slight modifications in reaction time. Leaves were thoroughly washed with tap water thrice to remove soil and dirt particle followed by washing with distilled water twice. The excess water was soaked into tissue paper and the leaves were left for oven drying in a hot air oven at 40°C. The dried leaves were ground finely. A ten gram of the powdered leaves was added to 100 ml of distilled water and heated at 60°C on a hot plate for 20 minutes, cooled at room temperature, and filtered through the mesh to remove the plant material. The extract solution was then centrifuged at 10000 rpm for 10 minutes and the clear supernatant was separated, filtered through Whatman Filter paper (No. 1), and finally stored in the refrigerator to avoid decomposition and fungal growth.

### 2.3.Preparation of metal salt solution

100 ml of 1 mM aqueous Gold (III) chloride trihydrate ($HAuCl_4. 3H_2O$) solution was prepared and stored away from dust.

### 2.4.Biosynthesis and optimization of reaction parameters

#### 2.4.1. Biosynthesis

At room temperature, the leaves extract was added to the 1 mM salt solution very slowly (drop-wise) and the final mixture was swirled for few minutes to ensure thorough mixing. The synthesized gold nanoparticle solution was centrifuged to separate the pellets and then washed with distilled water followed by ethanol several times to remove impurities. The separated pellets were dried at 60°C in a hot air oven. The remnant was then scraped out and ground finely into powder in a mortar with pestle. The obtained powder was weighed and stored.

#### 2.4.2.Optimization of reactants ratio

To determine the best ratio for synthesis and maximum yield under set experimental conditions, reaction mixtures were prepared with different ratios of extract and metal (1:9, 2:8, 3:7, 4:6, 5:5, 6:4, 7:3, 8:2, 9:1). The standard Surface Plasmon Resonance (SPR) of gold is between wavelength 500-550 nm [25]. The ratio which showed the highest absorbance in UV-Visible spectroscopy was

chosen for larger volume synthesis.

### 2.4.3. Optimization of reaction time

The minimum time that is required to complete the synthesis with maximum yield was optimized by taking a time-dependent UV-Visible Spectroscopy of the sample. The hour after which there was no further increase in absorbance of the reaction solution was fixed as the optimum reaction time.

### 2.5.Characterization of synthesized AuNPs

The UV Visible Spectroscopy (UV Visible spectrophotometer, Shimadzu, Japan, UV- 2400PC Series) was carried out to confirm and monitor the synthesis of AuNPs in an aqueous solvent in a wavelength range of 200-800 nm. The particle size was analyzed in a Particle Size analyzer (DLS) (Zetasizer version 6.12, Malvern Instruments Ltd.) to ensure the particles are formed below 100 nm. The size, crystalline structure and diffraction pattern were analyzed in X-ray diffractometer (XRD, PANalytical X'pert Pro). The Fourier Transform Infra-red Spectroscopy (FTIR) (Thermo Nicolet Model 6700) study was carried out for both the leaf powder and the synthesized AuNPs to probe the possible biomolecules responsible for bio-reduction. To determine the size, shape and morphology the particles were analyzed in SEM (JEOL Model JSM-6390LV) and Transmission Electron Microscopy (TEM, TECNAI-G2 F30-F TWIN). The elemental profile was demonstrated by the TEM- equipped Energy dispersive spectroscopy (EDAX) and Selected Area Electron Diffraction (SAED) pattern gives an insight into the crystallographic profile of the particles. The graphs of XRD and UV-Vis Spectroscopy were prepared from raw data using OriginPro 8.5 (Version 85E) Software.

### 2.6.Cytotoxicity Study

The cell viability study was performed with MTT-reduction assay to evaluate the efficacy of biosynthesized AuNPs against HCT 15 colon cancer cell line. The MTT (3-4,5-dimethylthiazol-2-yl)-2,5-diphenyltetrazolium bromide) tetrazolium reduction assay was adopted for the cytotoxicity test.

### 2.6.1. Cell line culture and MTT assay

The HCT15 cells were plated separately in 96-well plate with the concentration of $1\times10^4$ cells/well in DMEM media. Ten percent of antibiotic Solution and 10% of fetal bovine serum (FVS) was added to it. The cells were incubated at 37˚C in a $CO_2$ incubator (5% $CO_2$) for 24 h. The cells were washed with 200 µL of 10% Phosphate Buffer Solution (PBS). Different test concentrations of the gold nanoparticles viz., 25, 50, 100, 250 and 500µg/ml were added to the cells. The medium was aspirated from cells at the end of the incubation period of 24 hours. MTT (0.5mg/mL prepared in 10% PBS) was added to the cells and incubated at 37˚C for another 4 hours. The formed formazan crystals were dissolved with 100 µL of DMSO and thoroughly mixed. The development of color intensity was evaluated at 570nm. The absorbance of the purple formazan was measured in a microplate reader at 570 nm wavelength. Normal lymphocyte cells untreated with gold nanoparticles was set as the control.

## 3. RESULTS AND DISCUSSION

### 3.1. Visual observation and UV- visible spectroscopy

The biosynthesis of gold nanoparticles using the leaves extract of *W. trilobata* was carried out at room temperature and the reduction had happened within 30-35 minutes. The formation of the particles was confirmed by observing the change of colour (Figure 1) from light yellow to deep purple which develops due to the surface plasmon resonance of the formed particles and further confirmed by SPR peak around 530 nm in UV-Visible spectroscopy [21]. The ratio of 1:9 of extract and metal salt solution showed the highest absorbance of 2.9 at 533 nm (Figure 2). The absorption spectra showed an increasing trend in intensity up to six hours without showing any major shifts in SPR wavelength which states that the formed particles were stable. After 6 h the particles showed a decrease in absorbance (Figure 3).

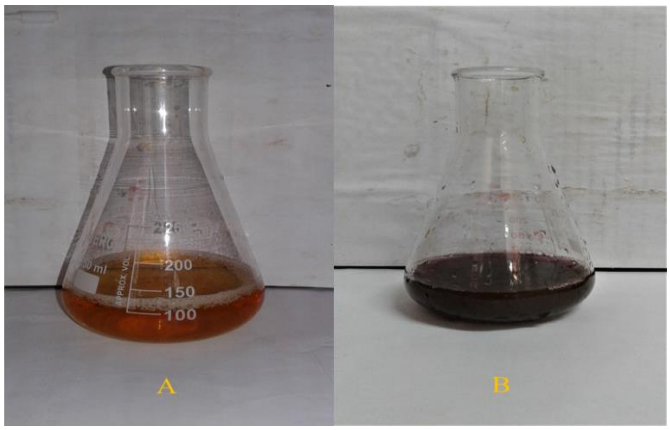


**Figure 1:** Reaction of aqueous *Wedelia trilobata* leaves extract with 1 mM $HAuCl_4$ solution. (A) At the beginning of the reaction; (B) deep purple colour formation after the addition of 1mM $HAuCl_4$ solution after 30 min of incubation.

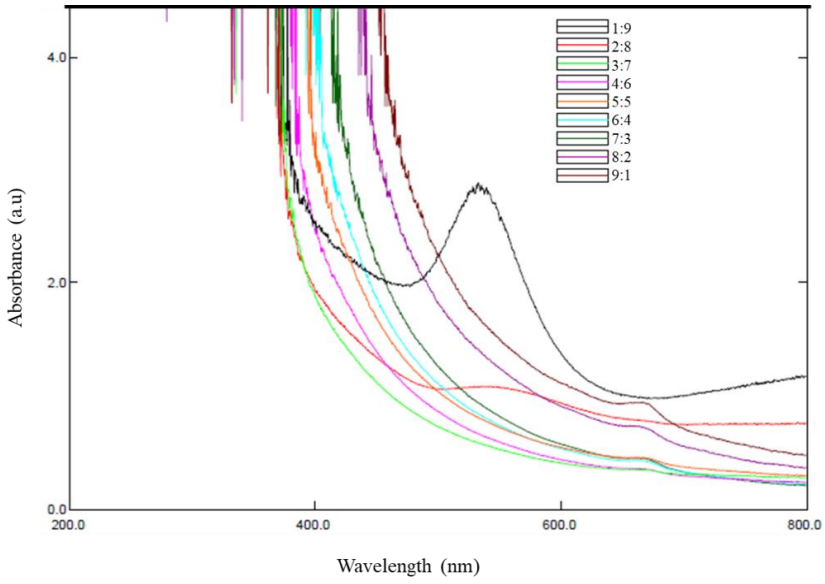


**Figure 2:** UV-Vis spectra recorded for gold nanoparticles in an aqueous solvent for nine different concentration ratios of extract and metal salt solution showing the highest absorbance of 1:9 ratio at 533 nm wavelength.

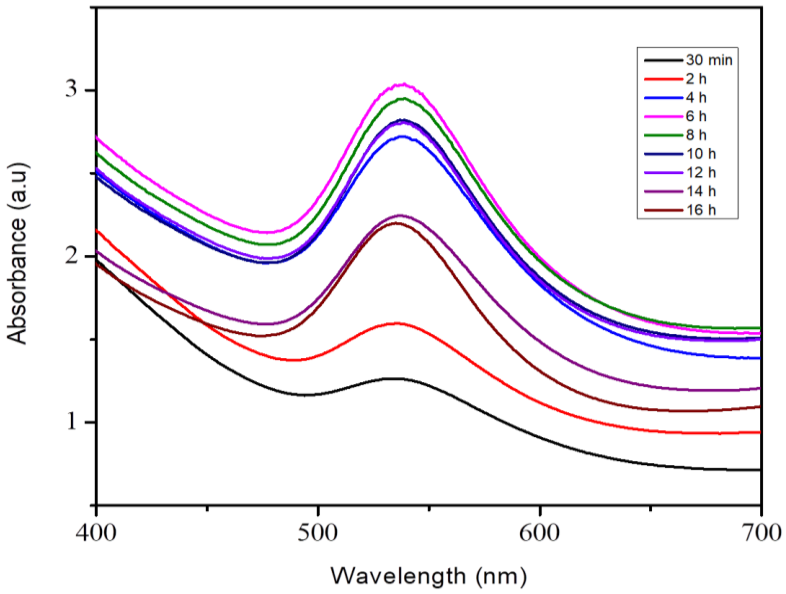


**Figure 3:** Time-dependent UV-Vis spectroscopy study of the prepared gold nanoparticles showing minimum reaction time of 30 mins and optimum time of synthesis to be 6 hours.

The optical absorption spectrum of the material was studied by Tauc relation [33,34] and the energy band gap estimated using Tauc plot (equation 1) was found to be 3.41 eV (Figure 4). The value is higher than the previously reported band gap energy of 2.95 and 2.90 [35] which may be attributed to the size of the nanoparticles.

$$\alpha h\nu = A(h\nu - Eg)^m \qquad (1)$$

Where A is optical constant, hυ is incident photon energy, α is the absorption coefficient, ($\alpha = 2.303 \times A/d$, where d and A are the width of the cell and absorbance, respectively). Eg is the band gap energy related to the particular transition in the materials. The exponent m has the value of ½, 3/2, 2, and 3 depending on the nature of the electronic transition.

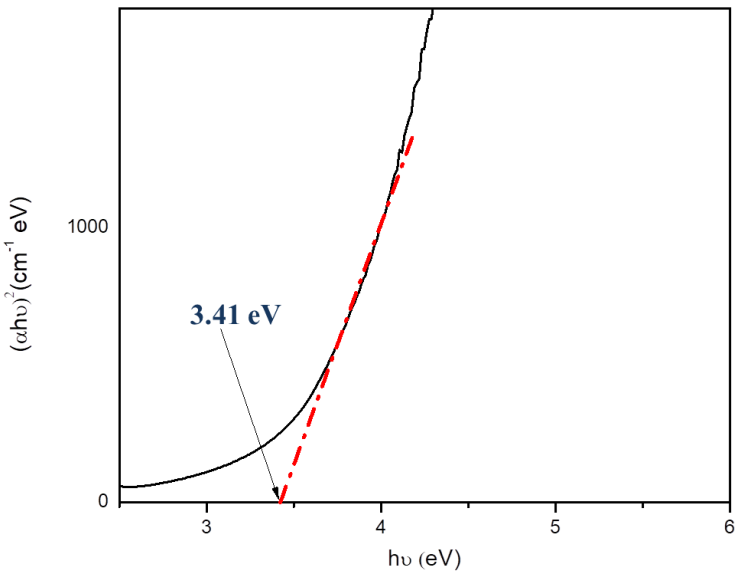


**Figure 4:** Band gap energy (eV) of the synthesized gold nanoparticles calculated using Tauc plot.

### 3.2. DLS

The hydrodynamic size for the synthesized nanoparticles in a solution of ratio 1:9 showed maximum particles size distribution in the size range of 6-10 nm (mean number 82.6 %) (Figure 5).

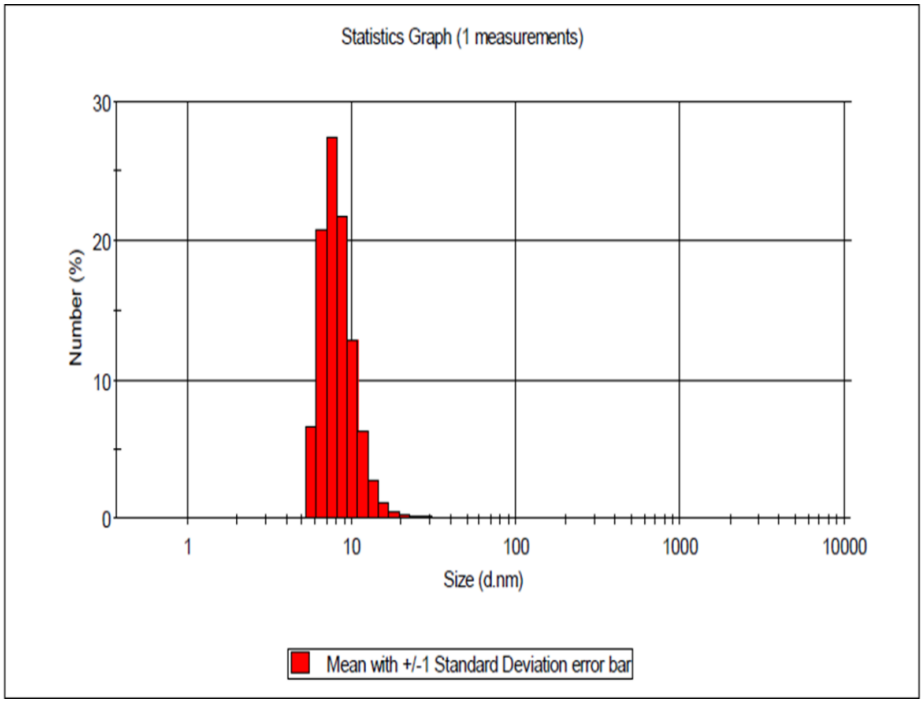


**Figure 5**: Dynamic Light Scattering showing particle size distribution (%) with maximum particles lying between the size ranges of 6-10 nm (82.6 %).

### 3.3.X-ray Powder Diffraction (XRD)

The XRD was carried out to confirm its crystallinity and structural phase analysis. The diffraction pattern with the wavelength of the light source at CuK-Alpha: (λ=0.154056 Angstrom) is shown in figure 6. The Bragg reflections were observed at 2θ=38.17º, 43.62º, and 64.60º corresponding to the lattice planes of (111), (200), and (220) (JCPDS 01-1174) for the face-centered cubic (fcc) metallic gold. A similar finding was reported by Ghodake et al. [39], Noruzi et al. [17], Reddy et al. [40], and Singh et al. [3]. The ratio of intensity between the planes confirms the preferred orientation of the particles in (111) plane characteristic of fcc crystalline structure [41]. In addition to these reflection peaks, a number of unassigned peaks were observed which can be attributed to the presence of salt residues and bio-organic phases on the surface of the Au nanoparticles [22] due to the impurities left during the post-synthesis isolation of nanoparticles. The inter-planar spacing (d-spacing) of the synthesized particles was calculated by using Bragg's diffraction equation.

$$2d \sin\theta = n\lambda \qquad (2)$$

Where d is inter-planar spacing, θ is Bragg's angle, n is the order of diffraction, and λ is the value of CuKα wavelength. The crystallite size was measured using Debye-Scherrer's formula.

$$t = 0.9\lambda/\beta \cos\theta \qquad (3)$$

Here, t is the crystallite size, and β denote full width at half maxima of the peaks for the lattice planes of the material. The d-spacing calculated was found to be 0.23 nm, 0.21 nm, and 0.14 nm for the planes (111), (200), (220) respectively corresponds to the standard Miller indices (JCPDS 01-1174). For the (111) plane of Au, the crystallite size was found to be 37.29 nm and average crystallite size was calculated to be 34.02 nm.

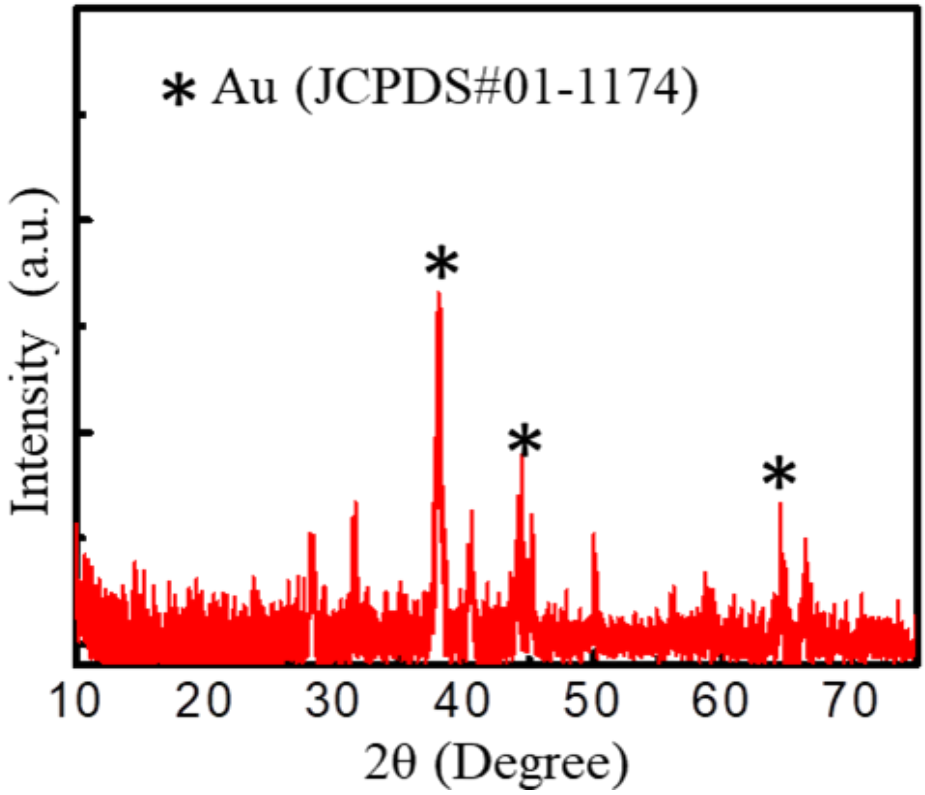


**Figure 6:** X-ray diffraction pattern of biosynthesized gold nanoparticles with the reference standard stick pattern of the elements presents. Peaks located at 38.17º, 43.62º, and 64.60º for the planes of (111), (200), and (220) respectively exhibiting the facets of crystalline gold.

### 3.4. Fourier Transform Infrared Spectroscopy (FTIR)

FTIR in the scan range of 400-4000 $cm^{-1}$ wavenumbers was carried out to identify the possible functional groups of the bioactive molecules taking part in the biosynthesis process. The FTIR spectra of plant extract and synthesized nanoparticles (Figure 7) shows strong and broad bonds between 3300-3444 $cm^{-1}$ corresponding to stretching vibrations of surface hydroxyl group (-OH) and can also be attributed to N-H stretching of the hydrogen-bonded amine group. The sharp peak at 1630 $cm^{-1}$ originates from C=O stretching vibrations in the amide linkages of proteins. The bond present between 1000-1100 $cm^{-1}$ in plant extract as well as in AuNPs arises due to C-OH and C-O epoxy group. The peak at 1397 $cm^{-1}$ for AuNPs arises due to the stretching vibrations of the C=C Carboxylic group. The sharp peak at 2927 and 2925 $cm^{-1}$ in AuNPs and leaves extract respectively is attributed to $–CH_2$ molecular stretching vibrations [36]. The relative shifts in peak intensity and position at 1441 $cm^{-1}$ and 1072 $cm^{-1}$ can be attributed to the surface binding of Polyphenolic groups onto the nanoparticles [37, 38].

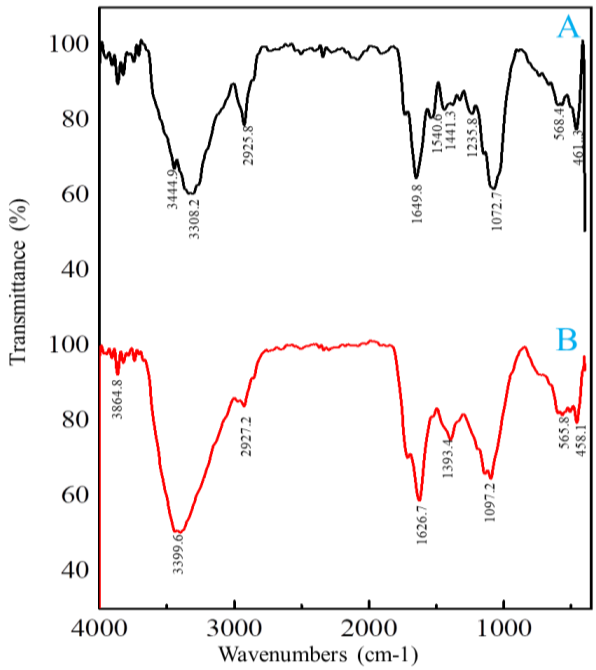


**Figure 7:** FT-IR spectrum of (A) Leaves extract and (B) synthesized nanoparticles showing shifting in peak intensity and position indicating the role of biomolecules in reduction and capping in nanoparticles synthesis.

### 3.5. Scanning Electron Microscopy (SEM)

SEM analysis was carried out to know the morphological feature of the particles which suggests that the particles are highly agglomerated and poly-dispersed in nature (Figure 8). The particles appeared as an aggregate of smaller particles embedded in biomatrix as suggested by Nadaf and Kanase (2016). The high degree of agglomeration may have happened due to an insufficient amount of capping agents on the surface of nuclei [42]. The extract ratio influences the formation of stable and symmetrical particles as well as aggregation behavior [43, 19]. Higher concentration of gold ions increases nucleation and thereby aggregation with increasing incubation time [44]. The synthesis and dispersion of nanoparticles in a highly polar solvent like water induces aggregation by hydrolytic reaction [45, 21].

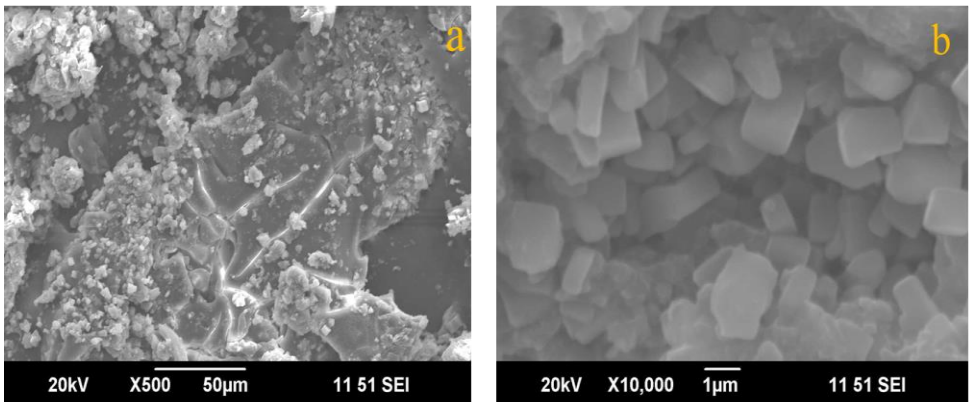


**Figure 8:** SEM images of AuNPs a. at X500 magnification & b) X10000 magnification showing the agglomerated distribution of the particles

### 3.6. TEM- SAED- EDAX

TEM observations were recorded from drop-coated films of gold colloids onto the carbon-coated copper grid. The particles are found to be predominantly spherical (Figure 9.A-9.C). The size of the particles ranges from 10 nm to 50 nm and the average size is calculated to be 39.76 nm. Lattice fringes with an inter-planar spacing of 0.24 nm were visible in TEM image (Figure 9.A). The fringe spacing matches with the d-spacing of (111) plane of the crystalline fcc Au (JCPDS card no 01-1174). A similar result was found by Majumdar et al. [38], Singh et al. [3], and Peter et al. [35]. The bright spots and spacing in SAED (Figure 9.D) indicated the crystalline nature of the as-prepared gold nanoparticles. The three bright rings correspond to the lattice planes of (111), (200), and (220).

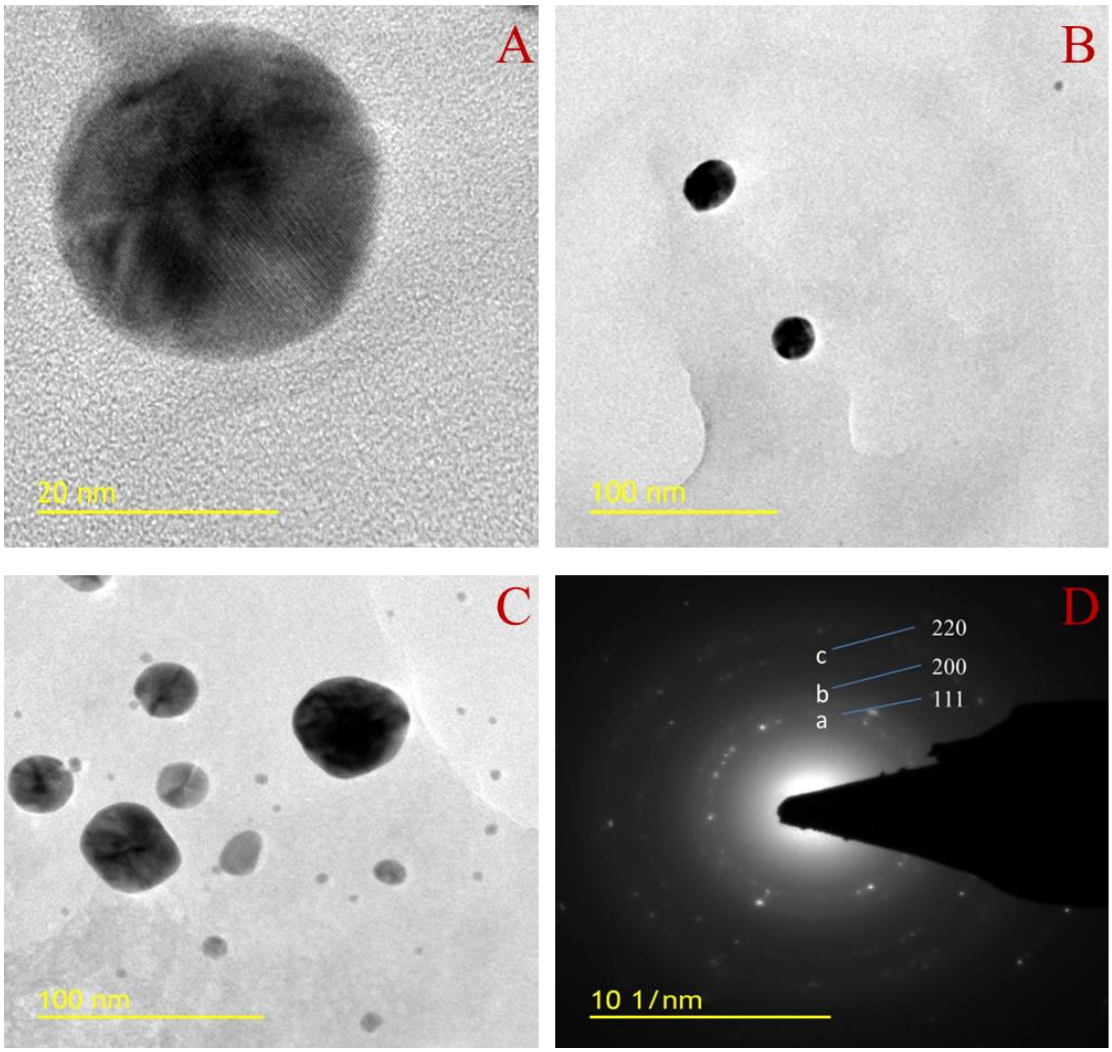


**Figure 9:** TEM images of bio-synthesized nanoparticles (A-C) on different nanometer scales showing the formation of spherical particles with an average size of 34.02 nm and (D) bright spots and rings in SAED indicating the lattice planes of the formed AuNPs crystals.

The EDAX measurements give the elemental composition profile of the synthesized particles. The presence of elemental Au observed in the graph (Figure 10) from EDAX analysis indicates the reduction of gold ions to elemental gold. In EDAX, a strong optical absorption peak was observed at 1.66 keV, 2.08 keV, 9.58 keV which is the characteristic peak for crystalline gold nanoparticles

and supported by previous literature [25, 46, 3, 22, 24]. Additional signals from carbon and copper appear due to the carbon-coated copper grid used for imaging the sample [3].

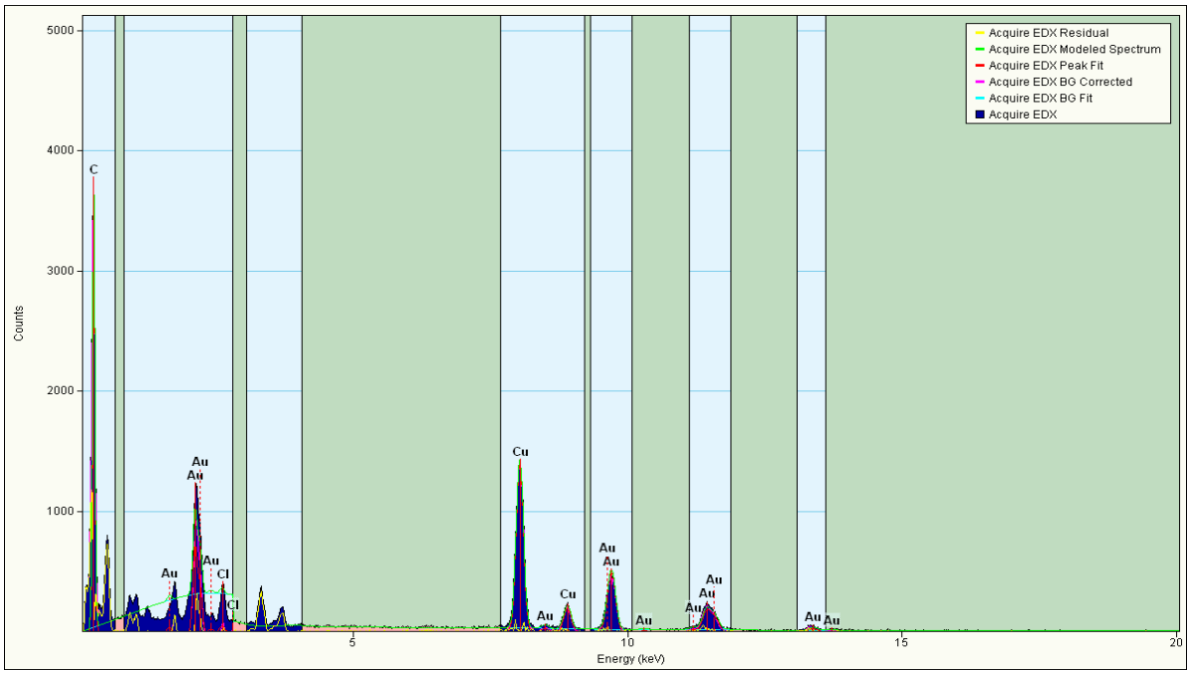


**Figure 10:** EDAX spectrum of prepared gold nanoparticles showing the peaks for major elements present. The strong peaks for Cu and C appear due to the Carbon-coated Copper grid used during sample loading.

### 3.7. Cytotoxicity assay

HCT 15 cells treated with AuNPs did not show significant toxicity in the test concentration range (25-500 µg/ml). The concentration of 500µg/ml showed cell toxicity of about 30% (Figure 11). Metabolically active cells convert MTT into a purple formazan with maximum absorbance at 570 nm. Only the viable cells can convert MTT into formazan. The development of purple colour thus acts as a marker of the live cells (Figure 12). The cellular mechanism of MTT reduction into formazan involves reaction with an enzyme in the mitochondria of live cells [47]. The cell viability showed dose-dependent cytotoxicity with the toxicity increasing with the increasing concentration of AuNPs [48, 49]. The cell viability percentage was calculated from the following formula.

$$\%\ of\ \ cell\ \ viability = \left[OD_{sample} - OD_{control}\ \right] \times 100/OD_{control} \qquad (4)$$

Here, OD is optical density at 570 nm

The data represents a percentage of cell viability of three independent experiments for each concentration and the solvent control. Cells exposed with 500 µg/ml gold nanoparticles showed almost 30 % of cell toxicity.

The cell toxicity is induced by apoptosis which is broadly considered as a programmed death of cells without any inflammatory response to healthy cells [49, 50]. As previously reported, the cytotoxicity of the gold particles is due to the interaction of the metal atoms with the functional

groups in intracellular proteins, nitrogen bases and phosphate groups in the DNA resulting in cell destruction [47]. The apoptosis mechanism involves fragmentation of DNA ladders associated with caspase-3 cascade activation. The increased activity of cascade-3 is mediated by the presence of toxic elements in cells and through granzyme B activation [51, 50, 26, 52, 49, 53]. The moderate level of cytotoxicity could be due to the agglomeration of the particles as cellular uptake of nanoparticles is dependent on their size, shape, concentration, type of cell, agglomeration status and surface chemistry, as well as experimental system variables like temperature, incubation time, and culture media [30, 54, 55, 56, 57, 58, 59].

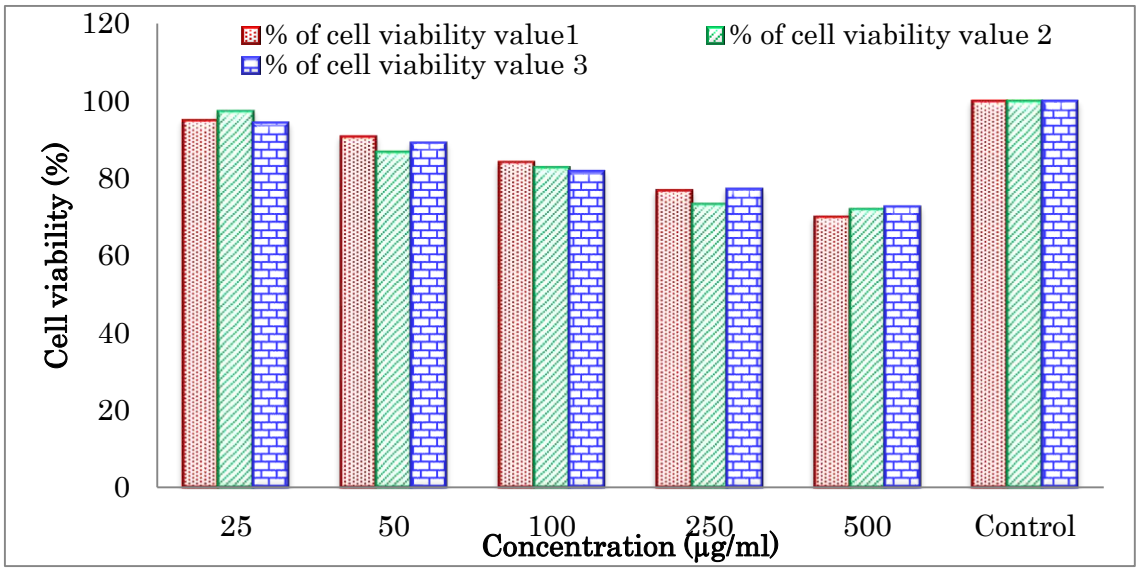


**Figure 11:** Cytotoxic effect of biosynthesized gold nanoparticles. HCT 15 Colon cells were treated with five different concentrations of nanoparticles and cell viability was determined by MTT assay.

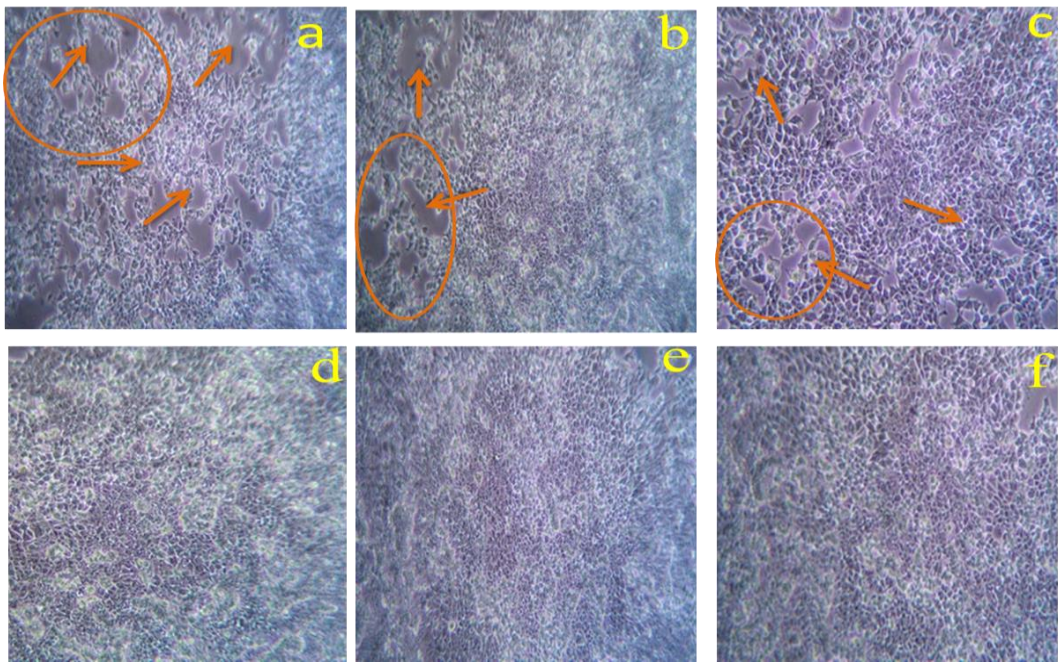


**Figure 12:** Microscopic images of HCT cells after treating with AuNPs in MTT assay at different concentrations a. 500 µg/ml, b. 250 µg/ml, c. 100 µg/ml, d. 50 µg/ml, e. 25 µg/ml, and f. Control

## 4. CONCLUSION

In the present study, gold nanoparticles have been prepared by biosynthetic route and the effect of reaction time as well as reactants volume ratio was observed. The ratio 1:9 of gold salt to extract with incubation for 12 hours was found optimum for synthesis. Spectroscopic and diffraction studies confirmed the crystalline nature and spherical shape with average size well below 100 nm. Studies could be taken up to enhance the cytotoxic efficiency of gold nanoparticles with suitable adjuvants.

## ACKNOWLEDGMENT

The authors would like to thank UGC for the fellowship and CIF, PU, for providing DLS, FTIR and TEM facility. The authors are grateful to the Head, Department of Earth Sciences, PU for providing XRD facility as well as STIC, CUSAT, Cochin for the SEM characterization. The authors would also like to acknowledge the support provided by the Pondicherry Centre for Biological Sciences (PCBS) to carry out the cytotoxicity assay.

## CONFLICT OF INTEREST

Authors declared that there is no conflict of interest.

## REFERENCES

1. Salam HA, Rajiv P, Kamaraj M, Jagadeeswaran P, Gunalan S. and Sivaraj, R. Plants: Green route for nanoparticle synthesis. International Research Journal of Biological Sciences 2012; 1(5): 85-90.
2. Lee KG, Hong J, Wang KW, Heo NS, Kim DH, Lee SY, Lee SJ, and Park TJ. In vitro biosynthesis of metal nanoparticles in microdroplets. ACS Nano. 2012; 6(8): 6998-7008.
3. Singh P, Kim YJ, Wang C, Mathiyalagan R, and Yang DC. The development of a green approach for the biosynthesis of silver and gold nanoparticles by using Panax ginseng root extract, and their biological applications. Artificial Cells, Nanomedicine, and Biotechnology. 2015; 44(4): 1150-1157.
4. Singh P, Kim YJ, Zhang D. and Yang DC, Biological synthesis of nanoparticles from plants and microorganisms. Trends in biotechnology, 2016; 34(7): 588-599.
5. Bar H, Bhui DK, Sahoo GP, Sarkar P, De SP, and Misra A, Green synthesis of silver nanoparticles using latex of Jatropha curcas. Colloids and Surfaces A: Physicochemical and Engineering Aspects, 2009; 339(1-3): 134-139.
6. Arunachalam KD, and Annamalai SK. Chrysopogon zizanioides aqueous extract mediated synthesis, characterization of crystalline silver and gold nanoparticles for biomedical applications. International Journal of Nanomedicine. 2013; 8: 2375.
7. Gardea-Torresdey JL, Parsons JG, Gomez E, Peralta-Videa J, Troiani HE, Santiago P, and Yacaman MJ. Formation and growth of Au nanoparticles inside live Alfalfa plants. Nano Letters. 2002; 2(4): 397-401.
8. Gardea-torresdey JL, Gomez E, Peralta-videa JR, Parsons JG, Troiani H, and Jose-yacaman M.

Alfalfa Sprouts : A Natural Source for the Synthesis of Silver Nanoparticles. Langmuir. 2003; (4): 1357–1361.

9. Shankar SS, Ahmad A, and Sastry M, Geranium leaf assisted biosynthesis of silver nanoparticles. Biotechnology Progress. 2003a; 19(6): 1627-1631.
10. Shankar SS, Ahmad A, Pasricha R, and Sastry M, Bioreduction of chloroaurate ions by geranium leaves and its endophytic fungus yields gold nanoparticles of different shapes. Journal of Materials Chemistry. 2003b; 13(7): 1822-1826.
11. Shankar SS, Rai A, Ahmad A, and Sastry M. Rapid synthesis of Au, Ag, and bimetallic Au core–Ag shell nanoparticles using Neem (Azadirachta indica) leaf broth. Journal of Colloid and Interface Science. 2004a; 275(2): 496-502.
12. Shankar SS, Rai A, Ankamwar B, Singh A, Ahmad A, and Sastry M. Biological synthesis of triangular gold nanoprisms. Nature Materials. 2004b; 3(7), pp.482-488.
13. Ankamwar B, Damle C, Ahmad A, and Sastry M. Biosynthesis of gold and silver nanoparticles using Emblica officinalis fruit extract, their phase transfer and transmetallation in an organic solution. Journal of Nanoscience and Nanotechnology. 2005; 5(10): 1665-1671.
14. Chandran SP, Chaudhary M, Pasricha R, Ahmad A, and Sastry M. Synthesis of gold nanotriangles and silver nanoparticles using Aloe vera plant extract. Biotechnology Progress. 2006; 22(2): 577-583.
15. Huang J, Li Q, Sun D, Lu Y, Su Y, Yang X, Wang H, Wang Y, Shao W, He N, and Hong J. Biosynthesis of silver and gold nanoparticles by novel sundried Cinnamomum camphora leaf. Nanotechnology. 2007; 18(10): 105104.
16. Song JY, Jang HK, and Kim BS. Biological synthesis of gold nanoparticles using Magnolia kobus and Diospyros kaki leaf extracts. Process Biochemistry. 2009; 44(10): 1133-1138.
17. Noruzi M, Zare D, Khoshnevisan K, and Davoodi D. Rapid green synthesis of gold nanoparticles using Rosa hybrida petal extract at room temperature. Spectrochimica Acta Part A: Molecular and Biomolecular Spectroscopy. 2011; 79(5): 1461-1465.
18. Gunalan S, Sivaraj R, and Venckatesh R. Spectrochimica Acta Part A : Molecular and Biomolecular Spectroscopy Aloe barbadensis Miller mediated green synthesis of mono-disperse copper oxide nanoparticles : Optical properties. Spectrochimica Acta Part A: Molecular and Biomolecular Spectroscopy. 2012; 97: 1140–1144.
19. Khalil MM, Ismail EH, El-Baghdady KZ, and Mohamed D. Green synthesis of silver nanoparticles using olive leaf extract and its antibacterial activity. Arabian Journal of Chemistry. 2014; 7(6): 1131-1139.
20. Rajakumar G, Gomathi T, Abdul Rahuman A, Thiruvengadam M, Mydhili G, Kim SH, Chung IM. Biosynthesis and biomedical applications of gold nanoparticles using Eclipta prostrata leaf extract. Applied Sciences. 2016; 6(8): 222.

21. Lee SY, Krishnamurthy S, Cho CW, and Yun YS. Biosynthesis of gold nanoparticles using Ocimum sanctum extracts by solvents with different polarity. ACS Sustainable Chemistry & Engineering. 2016; 4(5): 2651-2659.
22. Zha J, Dong C, Wang X, Zhang X, Xiao X and Yang X. Green synthesis and characterization of monodisperse gold nanoparticles using Ginkgo Biloba leaf extract. Optik-International Journal for Light and Electron Optics. 2017; 144: 511-521.
23. Barai AC, Paul K, Dey A, Manna S, Roy S, Bag BG, and Mukhopadhyay C. Green synthesis of Nerium oleander-conjugated gold nanoparticles and study of its in vitro anticancer activity on MCF-7 cell lines and catalytic activity. Nano Convergence. 2018; 5(1): 10.
24. Desai MP, Sangaokar GM, and Pawar KD. Kokum fruit mediated biogenic gold nanoparticles with photoluminescent, photocatalytic and antioxidant activities. Process Biochemistry. 2018; 70: 188-197
25. Siddiqi KS, and Husen A. Recent advances in plant-mediated engineered gold nanoparticles and their application in biological system. Journal of Trace Elements in Medicine and Biology. 2017; 40: 10-23.
26. Gurunathan S, Raman J, Malek SNA, John PA, and Vikineswary S. Green synthesis of silver nanoparticles using Ganoderma neo-japonicum Imazeki: a potential cytotoxic agent against breast cancer cells. International Journal of Nanomedicine. 2013; 8: 4399.
27. Zheng T, Bott S, and Huo Q. Techniques for accurate sizing of gold nanoparticles using dynamic light scattering with particular application to chemical and biological sensing based on aggregate formation. ACS Applied Materials & Interfaces. 2016; 8(33): 21585-21594.
28. Cai W, Gao T, Hong H, and Sun J. Applications of gold nanoparticles in cancer nanotechnology. Nanotechnology, Science and Applications. 2008; 1: 17-32
29. Priya MRK and Iyer PR. Anticancer studies of the synthesized gold nanoparticles against MCF 7 breast cancer cell lines. Applied Nanoscience. 2015; 7, 443–448.
30. Zăhan M, Muţoiu AM, Olenic L, Miclea I, Criste A, and Miclea V. Cytotoxic Effect of Chitosan-Gold Nanoparticles on Two Cell Lines in Culture. Bulletin UASVM Animal Science and Biotechnologies. 2017; 74: 2.
31. Govindappa M and Poojashri MN. Antimicrobial, antioxidant and *in vitro* anti-inflammatory activity of ethanol extract and active phytochemical screening of Wedelia trilobata (L.) Hitchc. Journal of Pharmacognosy and Phytotherapy. 2011; 3(3): 43-51.
32. Rather M, Pandian KJ, Sundarapandian SM and Yogamoorthi A. Biosynthesis and characterization of silver nanoparticles using leaf extract of Wedelia urticifolia (Blume) DC and evaluation of antibacterial efficacy. IOSR Journal of Pharmacy and Biological Sciences. 2017; 12 (4): 14-23
33. Tauc J, Grigorovici R and Vancu A. Optical properties and electronic structure of amorphous

germanium. Physica Status Solidi (b).1966; 15(2): 627-637.

34. Tauc J and Menth A. States in the gap. Journal of Non-crystalline Solids. 1972; 8: 569-585.
35. Peter J, Backialakshmi M, Karpagavinayagam P and Vedhi C. Green synthesis and characterization of colloidal gold nanoparticles for optical properties. Journal of Advanced Chemical Sciences. 2014; 1-5.
36. Jayaseelan C, Ramkumar R, Abdul A, and Perumal P. Green synthesis of gold nanoparticles using seed aqueous extract of Abelmoschus esculentus and its antifungal activity. Industrial Crops & Products. 2013; 45: 423–429.
37. Dzimitrowicz A, Jamróz P, Sergiel I, Kozlecki T and Pohl P. Preparation and characterization of gold nanoparticles prepared with aqueous extracts of Lamiaceae plants and the effect of follow-up treatment with atmospheric pressure glow microdischarge. Arabian Journal of Chemistry. 2016
38. Majumdar R, Bag BG and Maity N. Acacia nilotica (Babool) leaf extract mediated size-controlled rapid synthesis of gold nanoparticles and study of its catalytic activity. International Nano Letters. 2013; 3(1): p.53.
39. Ghodake GS, Deshpande NG, Lee YP and Jin ES. Pear fruit extract-assisted room-temperature biosynthesis of gold nanoplates. Colloids and Surfaces B: Biointerfaces. 2010. 75(2):.584-589.
40. Reddy V, Torati RS, Oh S and Kim C. Biosynthesis of gold nanoparticles assisted by Sapindus mukorossi Gaertn. Fruit pericarp and their catalytic application for the reduction of p-nitroaniline. Industrial & Engineering Chemistry Research. 2012; 52(2): 556-564.
41. Ankamwar B, Salgaonkar M, and Sur UK. Room temperature green synthesis of anisotropic gold nanoparticles using novel biological fruit extract. Inorganic and Nano-Metal Chemistry. 2017; 47(9): 1359-1363.
42. Nadaf NY and Kanase SS. Biosynthesis of gold nanoparticles by Bacillus marisflavi and its potential in catalytic dye degradation. Arabian Journal of Chemistry. 2016;
43. Sosa IO, Noguez C and Barrera RG. Optical properties of metal nanoparticles with arbitrary shapes. The Journal of Physical Chemistry B. 2003; 107(26): 6269-6275.
44. Yuan CG, Huo C, Yu S and Gui B. Biosynthesis of gold nanoparticles using Capsicum annuum var. grossum pulp extract and its catalytic activity. Physica E: Low-dimensional Systems and Nanostructures. 2017; 85: 19-26.
45. Martin MN, Basham JI, Chando P and Eah SK. Charged gold nanoparticles in non-polar solvents: 10-min synthesis and 2D self-assembly. Langmuir. 2010; 26(10): 7410-7417.
46. Geethalakshmi R and Sarada DVL. Gold and silver nanoparticles from Trianthema decandra: synthesis, characterization, and antimicrobial properties. International Journal of Nanomedicine. 2012; 7: 5375.
47. Rajeshkumar S. Anticancer activity of eco-friendly gold nanoparticles against lung and liver

cancer cells. Journal of Genetic Engineering and Biotechnology. 2016; 14(1): 195-202.

48. Muthukumar T, Sambandam B, Aravinthan A, Sastry TP and Kim JH. Green synthesis of gold nanoparticles and their enhanced synergistic antitumor activity using HepG2 and MCF7 cells and its antibacterial effects. Process Biochemistry. 2016; 51(3): 384-391.
49. Krishnaraj C, Muthukumaran P, Ramachandran R and Balakumaran MD. Acalypha indica Linn : Biogenic synthesis of silver and gold nanoparticles and their cytotoxic effects against MDA-MB-231, human breast cancer cells. Biotechnology Reports. 2014; 4: 42–49.
50. Franco JL, Posser T, Dunkley PR, Dickson PW, Mattos JJ, Martins R, Bainy AC, Marques MR, Dafre AL and Farina M. Methylmercury neurotoxicity is associated with inhibition of the antioxidant enzyme glutathione peroxidase. Free Radical Biology and Medicine. 2009; 47(4): 449-457.
51. Allen RT, Hunter III, WJ and Agrawal DK. Morphological and biochemical characterization and analysis of apoptosis. Journal of Pharmacological and Toxicological Methods. 1997; 37(4): 215-228.
52. Jänicke RU, Sprengart ML, Wati MR and Porter AG. Caspase-3 is required for DNA fragmentation and morphological changes associated with apoptosis. Journal of Biological Chemistry. 1998; 273(16): 9357-9360.
53. Moaddab S, Ahari H, Shahbazzadeh D, Motallebi AA, Anvar AA, Rahman-Nya J and Shokrgozar MR. Toxicity study of nanosilver (nanocid?) on osteoblast cancer cell line. International Nano Letters. 2011; 1(1): 11.
54. Sasidharan, A. and Monteiro-Riviere, N.A., 2015. Biomedical applications of gold nanomaterials: opportunities and challenges. Wiley Interdisciplinary Reviews: Nanomedicine and Nanobiotechnology, 7(6), pp.779-796.
55. Tay CY, Setyawati MI, Xie J, Parak WJ and Leong DT. Back to basics: exploiting the innate physicochemical characteristics of nanomaterials for biomedical applications. Advanced Functional Materials. 2014; 24(38): 5936-5955.
56. Park MV, Neigh AM., Vermeulen JP, de la Fonteyne LJ, Verharen HW, Briedé JJ, van Loveren H and de Jong WH. The effect of particle size on the cytotoxicity, inflammation, developmental toxicity and genotoxicity of silver nanoparticles. Biomaterials. 2011; 32(36): 9810-9817.
57. Zook JM, MacCuspie RI, Locascio LE, Halter MD and Elliott JT. Stable nanoparticle aggregates/agglomerates of different sizes and the effect of their size on hemolytic cytotoxicity. Nanotoxicology. 2011; 5(4): 517-530.
58. Jiang W, Kim BY, Rutka JT and Chan WC. Nanoparticle-mediated cellular response is size-dependent. Nature Nanotechnology. 2008; 3(3): 145.
59. Chithrani BD, Ghazani AA and Chan WC. Determining the size and shape dependence of gold nanoparticle uptake into mammalian cells. Nano letters. 2006; 6(4): 662-668.